# Inclusion compounds with a sexipedal host. Crystal structures and thermal analysis of inclusion compounds of hexakis(3-hydroxy-3,3-diphenylprop-2-ynyl)benzene with methyl ethyl ketone, diethyl ketone and diethyl ether

**Susan A. Bourne,*[a] Katherine L. Gifford Nash[a] and Fumio Toda[b]**

[a] *Department of Chemistry, University of Cape Town, Rondebosch, 7700, South Africa*
[b] *Department of Applied Chemistry, Faculty of Engineering, Ehime University, Matsuyama 790, Japan*

**Inclusion compounds of hexakis(3-hydroxy-3,3-diphenylprop-2-ynyl)benzene with methyl ethyl ketone, diethyl ketone and diethyl ether have been prepared and characterised by single crystal diffraction and thermal analysis. Kinetic parameters and mechanisms for the desolvation reactions have been determined. These have been correlated with structural features.**

## Introduction

Over the last two or three decades, organic hosts that form inclusion compounds have attracted a great deal of interest.[1] These compounds are studied as models for the processes of molecular recognition *via* intermolecular interactions,[2] as well as for their abilities to store or separate guest molecules.[3]

Recently, the synthesis of a new host compound, hexakis(3-hydroxy-3,3-diphenylprop-2-ynyl)benzene **H1**, and the crystal structure of its dimethylformamide inclusion compound were reported.[4] This encompasses the principles of host design suggested by Weber[5] in that it contains bulky side chains, which pack leaving cavities, and six hydroxy moieties, which act as hydrogen bonding donors to the guest molecules.

A chiral modification of **H1**, (−)-hexakis[3-(*o*-chlorophenyl)-3-phenyl-3-hydroxyprop-1-ynyl] benzene has also been prepared,[6] and work is continuing on possible chiral separations using this compound.

Inclusion compounds of **H1** have been found to form in various host:guest ratios, often considerably richer in guest than is usually observed for organic hosts. We now report the crystal structures and thermal analysis of the inclusion compounds of **H1** with **1**: methyl ethyl ketone (1:3), **2**: diethyl ketone (1:2) and **3**: diethyl ether (1:2).

## Experimental

The inclusion compounds **1–3** were obtained by dissolving the host compound in an excess of the guest liquid. Single crystals suitable for X-ray diffraction were obtained by slow evaporation over a period of 2–3 weeks. Preliminary cell dimensions and space group symmetry were determined photographically. X-Ray diffraction data were then measured on an Enraf-Nonius CAD4 diffractometer using graphite-monochromated Mo-Kα radiation ($\lambda$ = 0.7107 Å) with the $\omega$–$2\theta$ scan mode. In all cases the crystals were unstable in air, so the crystals selected were sealed in Lindemann capillary tubes in order to minimise crystal deterioration. Three reference reflections were monitored periodically to check orientation and crystal stability. The data reduction included correction for Lorentz and polarisation effects but not for absorption. Crystal data and experimental details are listed in Table 1.

All the structures were solved by direct methods using SHELXS-86,[7] and refined by full-matrix least-squares using SHELXL-93,[8] refining on $F^2$. All non-hydrogen atoms of the host molecules were refined anisotropically; aromatic hydrogens were placed in geometrically calculated positions. In **2** and **3**, hydroxy hydrogens were located in difference electron density maps and allowed to refine independently with isotropic temperature factors.

One of the methyl ethyl ketone guests in **1** was refined anisotropically, the other two (labelled J and K) were modelled isotropically because of their high temperature factors. The diethyl ketone molecule in **2** was refined with anisotropic oxygen atom and isotropically modelled carbons. One of the end carbon atoms of the diethyl ether molecule **3** is disordered over two positions, with sight occupancy factors of 0.39 and 0.61. All the non-hydrogen diethyl ether atoms were refined anisotropically.

Atomic coordinates, bond lengths and angles, and thermal parameters have been deposited at the Cambridge Crystallographic Data Centre (CCDC). For details of the deposition scheme, see 'Instructions for Authors', *J. Chem. Soc., Perkin Trans. 2*, 1996, Issue 1. Any request to the CCDC for this material should quote the full literature citation and the reference number 188/16.

### X-Ray powder diffraction

The samples were packed in aluminium sample holders and the powder patterns were measured using a Philips vertical goniometer with Ni filtered Cu-Kα radiation ($\lambda$ = 1.5418). Step scans (0.1° $2\theta$, with 2 s counting times) were performed from 6 to 35° $2\theta$. Automatic receiving and divergence slits were used.

### Thermal analysis

Thermogravimetry (TG) and differential scanning calorimetry (DSC) were performed on a Perkin-Elmer PC7 series system. The crystals were removed from their mother liquor, blotted dry and crushed before analysis. Sample analysis was on 3–5 mg. The TG and DSC runs were carried out at 10 °C min$^{-1}$, over the temperature range 30–300 °C. The purge gas was dry nitrogen flowing at *ca.* 40 cm$^3$ min$^{-1}$. Data for the kinetics of desolvation were obtained from isothermal thermogravimetric experiments carried out at temperature intervals of 2–5 °C over the range 62–72 °C for **1**, 55–80 °C for **2**, and 55–75 °C for **3**. The resultant percentage mass loss *vs.* time curves were converted to fractional reaction ($\alpha$) *vs.* time curves. Various kinetic models[9] were fitted to the data. The model chosen was the one which, for the temperatures considered, most nearly approached linearity over the largest $\alpha$-range. Values of $k$ obtained were used to produce Arrhenius plots for estimation of the activation energies of desolvation.

**Table 1** Crystal data and details of structure refinement

| Parameter | 1 | 2 | 3 |
|---|---|---|---|
| Molecular formula | $C_{96}H_{66}O_6 \cdot 3(C_4H_8O)$ | $C_{96}H_{66}O_6 \cdot 2(C_5H_{10}O)$ | $C_{96}H_{66}O_6 \cdot 2(C_4H_{10}O)$ |
| Molecular mass/g mol$^{-1}$ | 1531.80 | 1487.74 | 1463.72 |
| Crystal system | Monoclinic | Triclinic | Triclinic |
| Space group | $P2_1/c$ | $P\bar{1}$ | $P\bar{1}$ |
| $a$/Å | 12.320(5) | 10.912(4) | 10.651(1) |
| $b$/Å | 21.438(8) | 12.651(3) | 12.805(3) |
| $c$/Å | 32.92(2) | 15.705(4) | 15.560(4) |
| $\alpha$/° | 90.00(5) | 78.78(3) | 78.06(2) |
| $\beta$/° | 100.16(5) | 87.94(3) | 86.09(2) |
| $\gamma$/° | 90.00(3) | 76.42(3) | 76.12(1) |
| $V$/Å$^3$ | 8558(7) | 2070(17) | 2020(12) |
| $Z$ | 4 | 1 | 1 |
| $D_c$/g cm$^{-3}$ | 1.189 | 1.195 | 1.206 |
| $D_{obs}$/g cm$^{-3}$ | 1.154 | 1.170 | 1.185 |
| Linear absorption coefficient $\mu$/mm$^{-1}$ | 0.074 | 0.074 | 0.075 |
| $F(000)$ | 3240 | 786 | 774 |
| Colour | Pale yellow | Pale yellow | Colourless |
| Data collection | | | |
| $T$/K | 248(2) | 293(2) | 223(2) |
| Size of crystal/mm | 0.48 × 0.40 × 0.20 | 0.47 × 0.47 × 0.22 | 0.5 × 0.5 × 0.5 |
| Range scanned $\theta$ (°) | 1–25 | 1–25 | 1–25 |
| Range of indices $h$, $k$, $l$ | ±14, 25, 39 | ±12, ±15, 18 | ±12, ±15, 18 |
| Number of unique reflections collected | 15 742 | 7532 | 7367 |
| Number of reflections observed with $I_{rel} > 2\sigma I_{rel}$ | 8239 | 4416 | 5780 |
| Exposure time/h | 272 | 53.7 | 48.9 |
| Decay of standard reflections (%) | 21.0 | 0.2 | 2.6 |
| Final refinement | | | |
| $R$ ($I_{rel} > 2\sigma I_{rel}$) | 0.0891 | 0.0593 | 0.0484 |
| $wR2$ ($I_{rel} > 2\sigma I_{rel}$) | 0.2230 | 0.1503 | 0.1345 |
| $w$ [a] | $a = 0.1344$ $b = 16.85$ | $a = 0.0788$ $b = 1.20$ | $a = 0.0803$ $b = 0.70$ |
| $S$ | 1.018 | 1.013 | 1.034 |
| Mean shift/esd | 0.014 | 0.013 | 0.004 |
| Max. height in difference electron density map/e Å$^{-3}$ | 0.579 | 0.387 | 0.622 |
| Min. height in difference electron density map/e Å$^{-3}$ | −0.662 | −0.425 | −0.252 |

[a] $w = 1/[\sigma^2(F_o^2) + (aP)^2 + bP]$ where $P = [\max(F_o^2, 0) + 2F_c^2]/3$.

## Results and discussion

### Crystal and molecular structure

The atomic labelling used in **1–3** is shown in Scheme 1. All bond lengths and angles lie within expected ranges.[10] Crystallographic data have been deposited.

A similar scheme of hydrogen bonding is observed in all these structures. Details of the hydrogen bonds are given in Table 2, and all contacts are illustrated in Fig. 1. Commonly, one host hydroxy moiety acts as a hydrogen bond acceptor for another host hydroxy and at the same time, is a hydrogen bond donor to the guest's oxygen. In **1**, there are two exceptions: a hydrogen bond between O-5 and O-1G and a short contact between O-2 and the centroid of an adjacent phenyl ring in the same molecule [O-2 • • • centroid = 3.446(7) Å].

Compounds **2** and **3** are isostructural. The host molecules pack in layers with the central aromatic ring parallel to [110]. The diethyl ketone and diethyl ether guests are placed in cavities within these layers, between adjacent host molecules (Fig. 2). An examination of the volume occupied by the guest molecules showed that these cavities are approximately 7 × 9 × 8.5 Å.

Compound **1** crystallises in the space group $P2_1/c$, and the host molecules are packed not in layers, but with the planes of their central ring perpendicular to one another. This causes the methyl ethyl ketone guests to be situated in channels. Guest G is in a restricted channel parallel to [010], which is 2.3 Å at its narrowest point. The dimensions of the channel where this guest is situated are approximately 6 × 8 × 10 Å. Guest J is in a channel parallel to [100], which is centred at $z = 0.1$. The width of this channel in $z$ is 6.8 Å and in $y$ ranges between 5.5 and 7.7 Å. Guest K is in a zig-zag channel, which is approximately parallel to [100] and is centred at $z = 0.5$. The dimensions of this channel parallel to [010] and [001] are 7.5 and 8.8 Å, respectively.

### X-Ray powder diffraction

X-Ray powder diffraction data were collected for **1–3**, as well as for the desolvation products in each case. From these diffraction patterns it is clear that each compound on desolvation undergoes a phase change. The resulting desolvated pattern in each case matches that of the uncomplexed host material.

### Thermal analysis

TG was used to confirm the host : guest stoichiometry modelled in the crystal structures. Observed and calculated mass losses are shown in Table 3, and agree to within 1%.

Fig. 3 shows the TG and DSC curves for **2**, which is typical for all three compounds. DSC traces show a small, broad endotherm corresponding to the guest loss, followed by a sharper endotherm at 260 °C caused by the melting of the host. This is immediately followed by the exothermic decomposition of the host compound.

A series of isothermal TG experiments were carried out on **1** over a temperature range of 62–72 °C. An example of the resultant $\alpha$ *vs.* time curves is shown in Fig. 4. These curves were best described in two parts. The first part ($\alpha$-range 0–0.2) was linear. Then the Prout–Tomkins kinetic model fitted the second part of this reaction ($\alpha$-range 0.2–0.95). The semilogarithmic plot of ln $k$ *vs.* $1/T$, shown in Fig. 5, yields an activation energy of 156(9) kJ mol$^{-1}$.

The mechanism of guest release and structural collapse to the uncomplexed form for **2** and **3** is best described by the Avrami–Erofeev (A2) equation derived to model two-dimensional nucleation and growth of the product phase, and is charac-

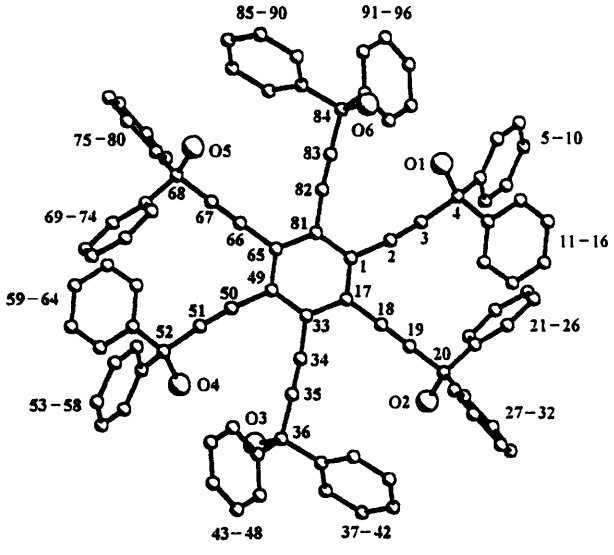


H1

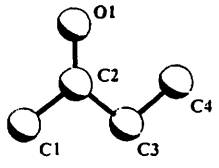


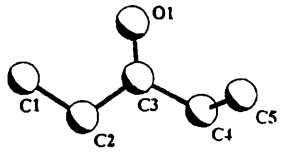


GUESTS LABELLED : G, J, K

1 2

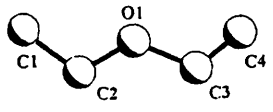


3

**Scheme 1**

**Table 2** Hydrogen bond data

| Compound | Donor | Acceptor | D–H/Å | D···A/Å | D–H···A (°) |
|---|---|---|---|---|---|
| 1 | O(1) | O(1)K[a] | | 2.665(8) | |
| | O(4) | O(1)J[b] | | 2.684(7) | |
| | O(5) | O(1)G[c] | | 2.807(6) | |
| | O(6) | O(1) | | 2.769(5) | |
| | O(3) | O(4) | | 2.834(5) | |
| 2 | O(2) | O(3) | 0.85(4) | 2.768(3) | 175(4) |
| | O(3) | O(1)G[d] | 0.80(4) | 2.69(2) | 165(4) |
| 3 | O(2) | O(1)[e] | 0.87(3) | 2.771(2) | 170(2) |
| | O(1) | O(1)G[f] | 0.84(3) | 2.690(2) | 162(2) |

[a] $1 + x, y, z$. [b] $x, 0.5 - y, -0.5 + z$. [c] $1 - x, -0.5 + y, 0.5 - z$. [d] $-x, 1 - y, 1 - z$. [e] $1 - x, 2 - y, 1 - z$. [f] $-x, 1 - y, 1 - z$.

**Table 3** Thermal analysis

| Compound | Calculated mass loss | Observed mass loss |
|---|---|---|
| 1 | 14.12 | 13.26 |
| 2 | 11.58 | 11.09 |
| 3 | 10.13 | 9.13 |

terised by sigmoidal $\alpha$ *vs.* time curves. An example of the $\alpha$ *vs.* time curves obtained for **2** over the temperature range 55–80 °C can be seen in Fig. 4. The curves are sigmoidal in shape

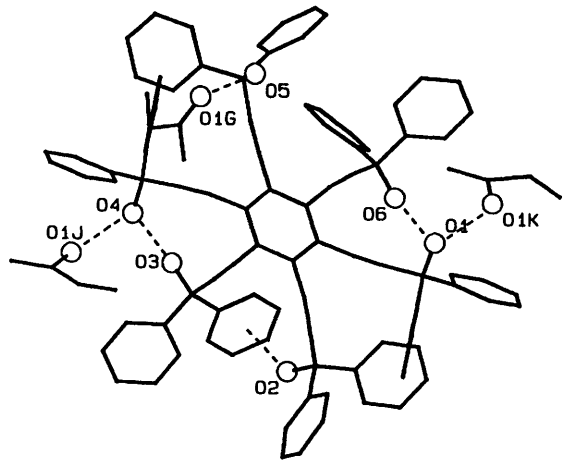


**Fig. 1** The hydrogen bonding scheme of compound **1**

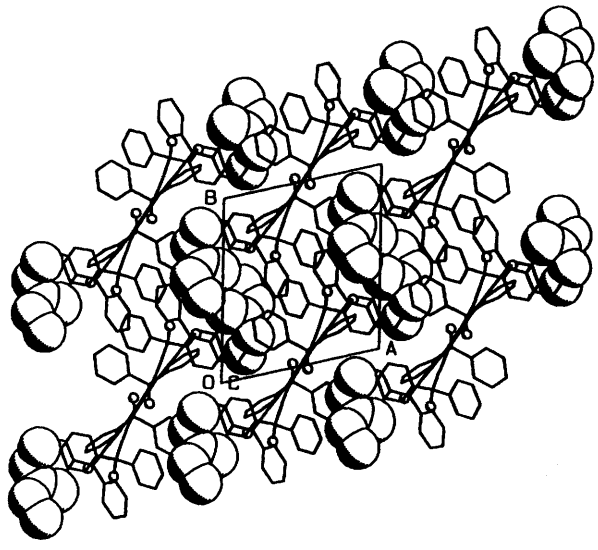


**Fig. 2** Crystal packing in compound **2** as viewed down [001]. The host is represented by stick figures, while the guests are shown as space-filled models.

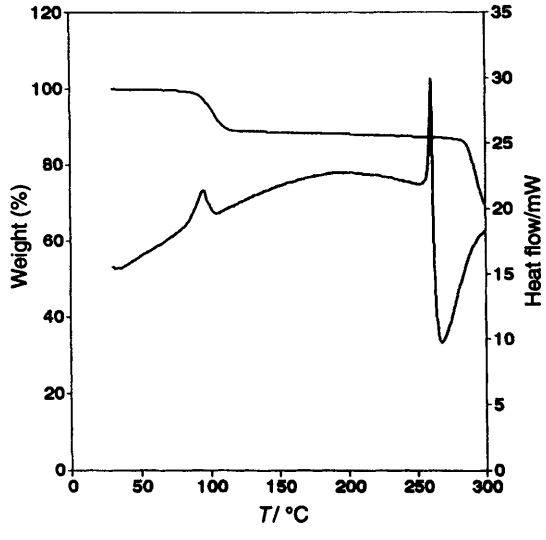


**Fig. 3** Thermograms showing the desolvation of compound **2**

clearly consisting of an induction period, an acceleratory stage and a deceleratory stage. An activation energy of 163(5) kJ mol$^{-1}$ was obtained for this reaction over an $\alpha$-range of 0.05–0.95. The semilogarithmic plot of $\ln k$ *vs.* $1/T$ is shown in Fig. 6.

An example of an $\alpha$ *vs.* time curve for **3** is also shown in Fig. 4.

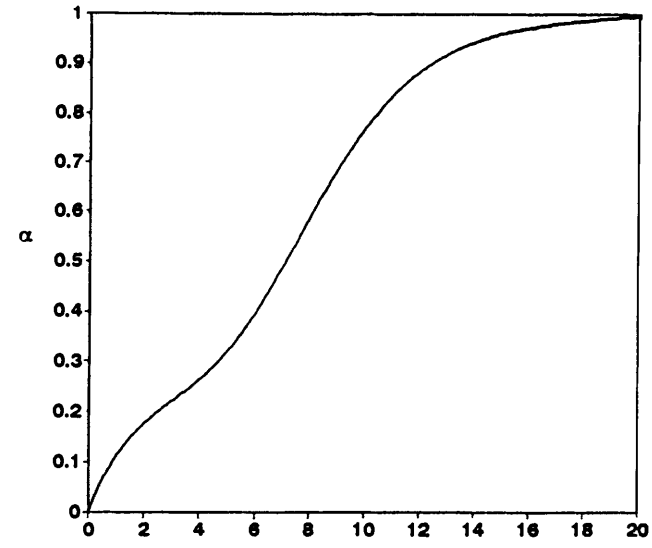


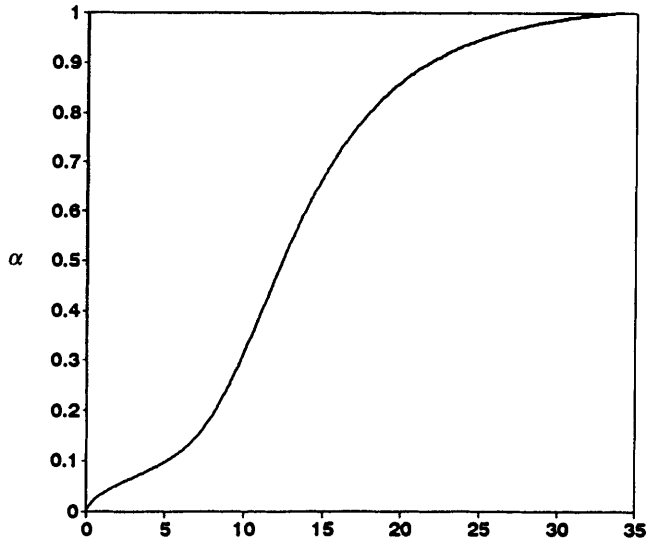


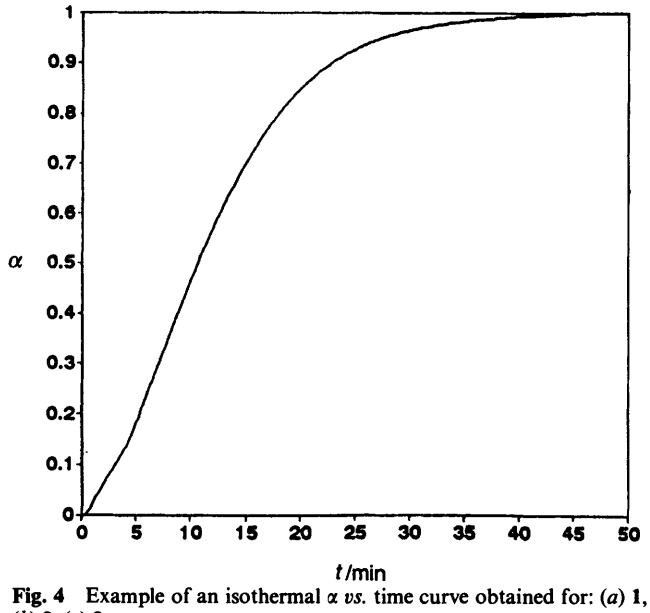


**Fig. 4** Example of an isothermal $\alpha$ *vs.* time curve obtained for: (*a*) **1**, (*b*) **2**, (*c*) **3**

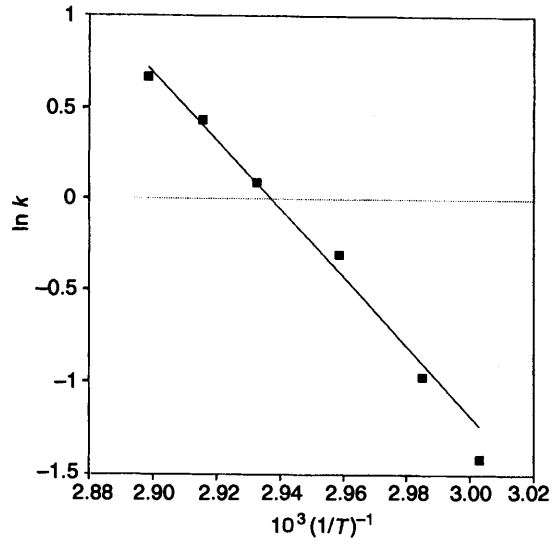


**Fig. 5** Arrhenius plot for the desolvation of compound **1**

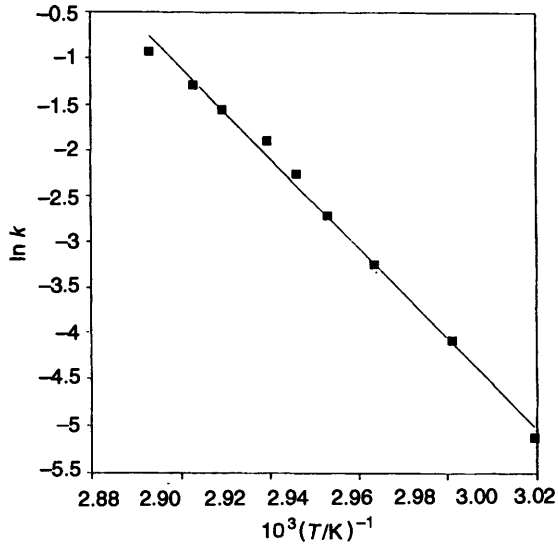


**Fig. 6** Arrhenius plot for the desolvation of compound **2**

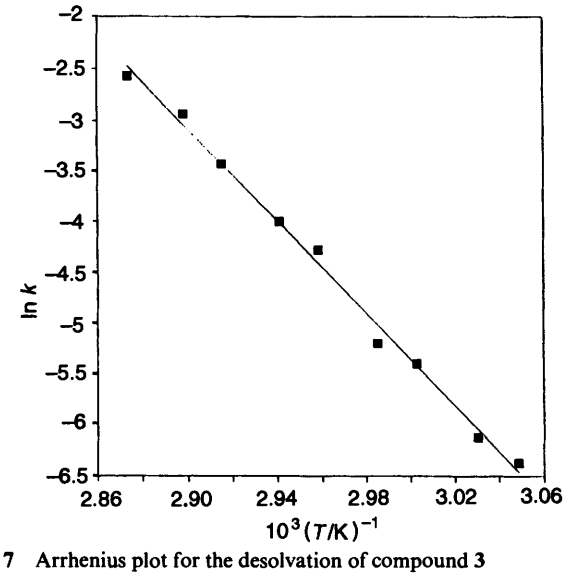


**Fig. 7** Arrhenius plot for the desolvation of compound **3**

These curves have a truncated sigmoidal shape since they did not possess a significant induction period, but consisted of an acceleratory and deceleratory section. An activation energy of 190(6) kJ mol$^{-1}$ was obtained over an $\alpha$-range of 0.05–0.95. The semilogarithmic plot of ln $k$ *vs.* $1/T$ is shown in Fig. 7.

It is apparent from the straight line nature of the Arrhenius plots that the guest release reaction: $HG(s) \rightleftharpoons H(s) + G(g)$, for each complex is isokinetic over the temperature ranges studied.

The activation energy of **1** is lower than that of both **2** and **3**, suggesting that the channels in **1** allow the gaseous decomposition product to escape more easily. **2** clearly has an induction period over the temperature range studied, implying that the initial rate of reaction is slow since the guest, which is captured in cavities cannot easily escape without disruption of the host framework. The rate of reaction then increases until a point of inflection is reached after which the curves become deceleratory. Although **2** and **3** are isostructural and the strengths of hydrogen bonds, as measured by the O···O distances, are similar in both, **3** has a greater activation energy than **2**. In a previous study,[11] we noted that for inclusion compounds of a given host with different guests, the onset temperatures ($T_{on}$) of the guest loss reactions are a function of both host–guest interactions and intrinsic physical properties of the guest. One of the most important of these is the normal boiling point ($T_b$) of the guest liquid. It was suggested that the temperature difference $T_{on} - T_b$ is a measure of the thermal stability of the inclusion compound. For **2**, this difference is −15 °C, while for **3** it is 43 °C. Thus, **3** appears more thermally stable than **2**, which may account for the difference in their activation energies of desorption.

## References


1 *Inclusion Compounds*, ed. J. L. Atwood, J. E. D. Davies and D. D. MacNicol. Academic Press, London, 1984, vols. 1–3; Oxford University Press, 1991, vol. 4.
2 *Molecular Inclusion and Molecular Recognition—Clathrates I and II. Topics in Current Chemistry*, ed. E. Weber, Springer-Verlag, Berlin, 1988 and 1989, vols. 140 and 149.
3 F. Toda, K. Tanaka and H. Ueda, *Tetrahedron Lett.*, 1983, **22**, 4669; F. Toda, K. Tanaka, H. Ueda and T. Oshima, *J. Chem. Soc., Chem. Commun.*, 1983, 743.
4 S. A. Bourne, M. R. Caira, L. R. Nassimbeni, M. Sakamoto, K. Tanaka and F. Toda, *J. Chem. Soc., Perkin Trans. 2*, 1994, 1899.
5 E. Weber, in ref. 1, vol. 4.
6 S. A. Bourne, M. Sakamoto and F. Toda, *J. Chem. Crystallogr.*, 1995, **25**, 755.
7 G. M. Sheldrick, *Acta Crystallogr., Sect A.*, 1990, **46**, 467.
8 G. M. Sheldrick, SHELXL-93, *J. Appl. Crystallogr.*, in preparation.
9 M. E. Brown, in *Introduction to Thermal Analysis, Techniques and Applications*, Chapman and Hall, London, 1988.
10 F. H. Allen, O. Kennard, D. G. Watson, L. Brammer, A. G. Orpen and R. Taylor, *J. Chem. Soc., Perkin Trans. 2*, 1987, S1.
11 S. A. Bourne, L. R. Nassimbeni and M. L. Niven, *J. Phys. Org. Chem.*, 1992, **5**, 769.



*Paper* 6/02503J
*Received* 10*th April* 1996
*Accepted* 29*th May* 1996